Green Chemistry

The Effects of Polyolefin Structure and Source on Pyrolysis-Derived Plastic Oil Composition

Journal:	*Green Chemistry*
Manuscript ID	GC-ART-08-2024-004029.R1
Article Type:	Paper
Date Submitted by the Author:	09-Oct-2024
Complete List of Authors:	Wu, Jiayang ; University of Wisconsin, Chemical and Biological Engineering Jiang, Zhen; Northwestern University, Chemical and Biomolecular Engineering ; 1989 Cecon, Victor; Iowa State University Curtzwiler, Greg; Iowa State University of Science and Technology, Polymer and Food Protection Consortium; Iowa State University of Science and Technology, Food Science and Human Nutrition Huber, George; University of Wisconsin-Madison, Department of Chemical and Biological Engineering Vorst, Keith; Iowa State Univ, Polymer and Food Protection Consortium Mavrikakis, Manos; University of Wisconsin Madison, Chemical and Biological Engineering

The Effects of Polyolefin Structure and Source on Pyrolysis-Derived Plastic Oil Composition

Author: Jiayang Wu[1], Zhen Jiang[1], Victor S. Cecon[2], Greg Curtzwiler[2], Keith Vorst[2], Manos Mavrikakis[1], George W. Huber[1]*

[1] Department of Chemical and Biological Engineering, University of Wisconsin-Madison; Madison, WI 53706, USA

[2] Polymer and Food Protection Consortium, Department of Food Science and Human Nutrition, Iowa State University, Ames, IA 50011, USA

*Corresponding authors: gwhuber@wisc.edu

Abstract

Seven types of plastics were pyrolyzed in a fluidized bed reactor: post-consumer recycled (PCR) high-density polyethylene (HDPE), PCR polypropylene (PP), virgin resins of varying molecular weights of HDPE, virgin resins of low-density polyethylene (LDPE), linear low-density polyethylene (LLDPE), and (PP). Pyrolysis produced non-condensable gases (C1-C3), liquid phase products (C4-C40), and solids (C40+ and chars), with alkane, alkene, alkadiene, aromatic, and multi-cycloaromatics as the predominant compounds. Polymer structure had the greatest impact on product distribution, with minimal influence from molecular weight. Branches in polyethylene (PE) acted as thermal defects initiating degradation. Higher branch density in PE led to increased concentrations of aromatics, branched alkanes, and internal alkenes. PP and PE exhibited distinct degradation mechanisms, with PP requiring less energy for decomposition and yielding more oil. Pyrolysis oil from PCR HDPE and PCR PP contained a higher proportion of branched compounds. Additives in PCR plastics may promote isomerization during pyrolysis.

1. Introduction

Nearly 4 billion tons of plastic waste were produced globally in 2022.[1] Plastic production is increasing at an annual rate of 3.3%, signifying a continual rise in plastic waste quantities.[2] The amount of accumulated discarded plastic could reach 12 billion tons by the end of 2050 if advanced recycling technologies are not rapidly developed and deployed.[2] In 2016, plastic wastes occupied 20 wt% of the total waste going into landfills.[3] In the United States (U.S.), polyolefins (polyethylene and polypropylene) represented 65 wt% of the total plastic waste in 2018, with a recycling rate of less than 3 wt%.[3] A wide variety of polyolefins are used in industry which are typically classified into four different classes: high-density polyolefins (HDPE), polypropylene (PP), low-density polyethylene (LDPE), and linear low-density polyethylene (LLDPE).[4, 5] Over a dozen different grades of these four different classes exist which have different molecular weights distributions, additives and colorants. The wide variety of polyolefins makes mechanical recycling of polyolefins very difficult as it involves a lot of sorting and cleaning.[6]

Plastic pyrolysis thermally decomposes polyolefins in an oxygen-free environment to small molecules. These small molecules can be upgraded back into virgin plastics or other valuable materials. By 2030, the plastic pyrolysis market is projected to reach $25.4 billion.[7] There are three potential methods to upgrade the plastic pyrolysis oils including: (1) blending with naphtha for olefin production in steam crackers,[8] (2) utilizing zeolites to produce short chain olefins and aromatics,[9] and (3) hydroformylating the pyrolysis oils to yield aldehydes, alcohols, carboxylic acids, and amines.[10, 11] Steam crackers and zeolite upgrading require low levels of alkenes in the feed because of coke formation. Alkene and alkadienes are desirable in hydroformylation of the pyrolysis oils to produce more valuable aldehydes and dialdehydes.[10] A more detailed understanding the chemistry of polyolefin pyrolysis and their product distributions could provide special insights for how to apply pyrolysis for upcycling of polyolefins.

Numerous studies on polyolefin pyrolysis have been reported in the academic literature. Kusenberg et al. reported a detailed study comparing the pyrolysis of real waste polyethylene (PE) film and polypropylene (PP) mixture through a continuous stirred tank reactor (CSTR). The products were

characterized using a two-dimensional gas chromatography (GC×GC) system, indicating that the PP-derived oil has a higher concentration of branched olefin and diolefins than the PE-derived oil .[12] Abbas-Abadi et al. studied virgin LDPE, virgin and waste PP, along with LDPE-rich polyolefin wastes under pyrolysis condition of 430 ~ 490 ^{0}C and pressure between 0.1 ~ 2 bar using a CSTR. The products were analyzed by GC×GC, demonstrating that increased pressure and temperature resulted in a higher yield of lighter products, alkenes and conjugated alkadienes.[13] These studies have a very thorough analysis with the pyrolysis oil compositions along with potential impurities.

Perez et al. investigated the degradation of virgin PP pyrolysis under three temperatures (460 ^{0}C, 530 ^{0}C, and 600 ^{0}C), three particles sizes (53 – 125, 125 – 300, and >300 μm), and three residence times (16, 24, and 48 ms) with a Frontier pyrolizer, with products quantification through GC×GC, and found there was no statistical difference between the products at these different conditions.[14] Krishna et al. applied the same reaction conditions and analytical tools to study virgin PE pyrolysis, reporting increased yields of cyclodiolefins, cycloolefins, and aromatics at 600°C.[15] Zhang et al., also using a Frontier pyrolizer, reported that the apparent activation energy for pyrolysis increased on the order of simulated plastic waste mix (a mix of virgin resins) < PP < PE. [16] The Frontier reactor typically requests very small sample amount (μm to mg level), requiring highly homogeneous samples, which made it difficult to apply to study the actual waste. The simulated plastic waste mix also cannot fully represent the actual plastic waste due to the presence of additives and contaminants such as pigments, paper, or aluminum films. Therefore, the results obtained from a Frontier pyrolizer cannot fully present industrial pyrolysis processes.

These studies illustrate that the products from plastic pyrolysis are complicated with more than 500 individual products. Plastic pyrolysis produces a broad range of molecular weights from light gases (methane) to heavy waxes (~ C70). The products include linear alkanes, iso-alkanes, linear alkenes, iso-alkenes, cyclic alkenes, linear alkadienes, conjugated-alkadienes, iso-alkadienes, cyclic-alkadienes, aromatics, and polycyclic aromatic hydrocarbons (PAHs).[8, 13-15, 17] Most of the previous studies were done with virgin polyolefins while impurities in post-consumer recycling (PCR) polyolefins could influence the reaction chemistry. More research is needed to better understand the complex chemistry that occurs during the pyrolysis of PCR polyolefins.

The objective of this paper is to provide a more detailed understanding of PCR polyolefin plastic pyrolysis chemistry using different PCR and virgin polyolefins feedstock combined with modern analytical methods and with density functional theory (DFT) calculations. This paper examines polyolefins pyrolysis using a continuous fluidized bed reactor, comparing three key factors: (1) the branching structure of polyolefins, (2) the molecular weight of the polymers, and (3) the source of the plastics (PCR vs. virgin grades). A detailed understanding of the pyrolysis oil was done using GC×GC, with alkene structures further identified through nuclear magnetic resonance (NMR). DFT calculations are combined with the experimental results to provide a mechanistically based understanding of the polyolefin degradation pathways. Seven types of polyolefins were tested: post-consumer recycled (PCR) HDPE, PCR PP, virgin HDPE with varying molecular weights, virgin LDPE, LLDPE, and PP. The feedstocks were characterized for their structural properties and impurities. Structural and branch density analyses of all plastics were conducted using NMR, attenuated total reflectance Fourier transform infrared spectroscopy (ATR-FTIR), and gel permeation chromatography (GPC). The pyrolysis products were evaluated using GC×GC with duo detectors of flame ionization detector (FID), and mass spectroscopy (MS), NMR, and inductively coupled plasma (ICP) spectroscopy.

The results indicate that the branching structure of polyolefins plays a significant role in the distribution of gas, liquid, and solid products, as well as in the oil composition and alkene structures, while molecular weight and impurities have the least impact on these factors. This is because a higher branch density in PE leads to decreased alkene yields and increased yields of alkanes and aromatics, with more

internal alkene structures reducing the likelihood of random scission reactions. PE and PP tend to degrade from the carbon backchain, whereas LDPE and LLPDE tend to cleave from branch structures.

2. Experiments

2.1 Materials

Seven types of plastic were used in this study: post-consumer recycled (PCR) high-density polyethylene (HDPE) and PCR polypropylene (PP) flakes, which were collected by Iowa State University (ISU); HDPE virgin resins with two different molecular weights (the one with high molecular weight is referred to as HDPE HMW, and the one with low molecular weight is referred to as HDPE LMW); low-density polyethylene (LDPE) virgin resins; linear low-density polyethylene (LLDPE) virgin resins; and PP virgin resins were received from Amcor. All plastics were shredded to approximately 3 mm particle size. Fig. S1 shows the PCR plastics fed into the fluidized bed reactor. All other chemicals used for GC calibrations and NMR were obtained from Sigma-Aldrich. Detailed information can be found in the SI material section. Table 1 lists the manufacturers and molecular weights of virgin polymers.

2.2 Pyrolysis and Distillation

The plastic was fed into a customized fluidized bed reactor and pyrolyzed at 500˚C with a residence time of 20 seconds and a plastic feeding rate of 2 g/min. We chose this reaction condition because it provided the highest oil yield without producing excessive heavy oil, which favors potential upgrading methods. The pyrolysis reactor operated for one hour. Pyrolysis oils were collected in 10 condensers arranged in series (4 condensers in an ice bath and 6 condensers in a dry ice bath), and the non-condensable gas was collected in gas bags every 10 minutes. The overall gas flow was measured using a 100 ml soap film flowmeter. After each pyrolysis run, the sand was removed, and approximately 60 g of sand was calcined in a muffle furnace at 600˚C for at least 3 hours to ensure all char was burnt out. The mass of the char was determined by the mass difference of the sand before and after calcination. The remaining sand was returned to the fluidized bed reactor and calcined in the reactor at 600˚C for 5 hours with an airflow. The collected pyrolysis oils were distilled into two fractions: light oil (C4-C10) and heavy oil (C10+) to simplify oil characterization. Detailed descriptions of the fluidized bed reactor and distillation process are provided in SI section 2.[10, 17]

2.3 Plastic and Plastic Oil Characterization

The plastics were characterized by ATR-FTIR (Bruker Vertex 70) and high-temperature quantitative NMR (Bruker Avance-500, with BBFO probe) before pyrolysis to check the purity of the polymers used, as well as the branch density of the polymers. These plastics were also analyzed with high-temperature GPC (Malvern Viscotek 350 HT-GPC) to obtain molecular weight data. TGA (TA Instruments Q5000IR thermogravimetric analyzer) was used to obtain the thermal degradation patterns of the polyolefins and compare them with the pyrolysis results. The pyrolyzed plastic oils (undistilled oil, light oil, and heavy oil) were characterized by GC × GC-FID (Agilent 7890B) and NMR (Bruker Avance-500 with a DCH cryoprobe). The gas samples collected in gas bags were characterized by a refinery gas analyzer (RGA) with both FID and TCD detectors (Shimadzu GC-2014). Both the plastics and their corresponding oils were digested using a microwave digestion system (Milestone UltraWave) and characterized by ICP-OES (Thermo Scientific iCap-7400 Duo) for trace elements (impurities) information. Detailed information is provided in ESI sections 3.1 to 3.6.

2.4 DFT Mechanistic Studies of Polyolefin Degradation

All calculations were performed using the Gaussian 09 software package.[18] High density polyethylene (HDPE) was modeled by an oligomer of $C_{10}H_{22}$ with linear C-backbone benchmarked in our previous study.[10] To consider the branch effects on the energetics of the C-C bond scission, five methyl

groups and one butyl group were initially added to our HDPE model as branches of PP and LLDPE oligomers, respectively (Fig.8A). More detailed information is provided in the ESI, section 3.7.

3. Results

3.1 Characterization of the Plastic Feedstocks

Fig.1A shows the ATR-FTIR spectra of PCR-HDPE, PCR PP and virgin polyolefins used for this study. The FTIR spectra of PCR HDPE and PCR PP were obtained from 10 random samples, with all PCR plastics' spectra illustrated in ESI Fig.S3. Three representative spectra of PCR HDPE and PCR PP are shown in Fig.1A. The PCR HDPE samples, sourced from Mexico by Iowa State University, primarily comprised ground detergent bottles. The PCR PP samples were obtained from a local Material Recovery Facility (MRF) in Iowa and exhibited higher impurity levels compared to the PCR HDPE samples, including alumina film, various fillers, and paper contaminants. The FTIR spectra of PCR HDPE showed four main peaks, identical to those of virgin HDPE resins: 2916 cm^{-1} and 2848 cm^{-1}, assigned to CH stretching in -CH_2- groups; 1467 cm^{-1}, assigned to C-H bending in CH_2 groups; and 721 cm^{-1}, attributed to the rocking mode of CH_2 groups. [19, 20] For the PCR PP FTIR spectra, two main groups of peaks were observed, which were also shown in the virgin PP resins: 2947 cm^{-1}, 2924 cm^{-1}, and 2846 cm^{-1}, assigned to CH_2 and CH_3 stretching; and 1448 cm^{-1} and 1379 cm^{-1}, assigned to symmetrical bending in CH_3 groups.[21]

FTIR analysis indicated the presence of trace amounts of other plastics, such as ethylene vinyl alcohol copolymer (EVOH) in PCR PP, due to the distinct peak at 3321 cm^{-1} in the PCR PP3 spectrum, which can be attributed to OH groups. Peaks observed at 1100 cm^{-1} and 1180 cm^{-1} in both PCR HDPE and PP spectra could be attributed to the fluorinated polyolefins containing CHF and CF_2 groups,[22, 23] as fluorination is commonly used in polyolefin containers to enhence chemical storage performance.[23]

Quantitative ^{13}C high temperature NMR was used to quantify the branch structure in all the polyethylene samples, as shown in Fig.1B. The peak shown in 14.02 ppm is assigned as the primary carbon, and the peak shown in 38.28 ppm is assigned as the tertiary carbon.[24, 25] Virgin and PCR HDPE plastics had no detectable branches, while LDPE contained 10 tertiary carbons per 1000 carbons, and LLDPE contained 20 tertiary carbons per 1000 carbons. Tertiary carbons refer to the carbons in the carbon backbones that have a branch. The ranking of polyethylene branch density in this study, from highest to lowest, is: LLDPE (2%) > LDPE (1%) > HDPE (0%).

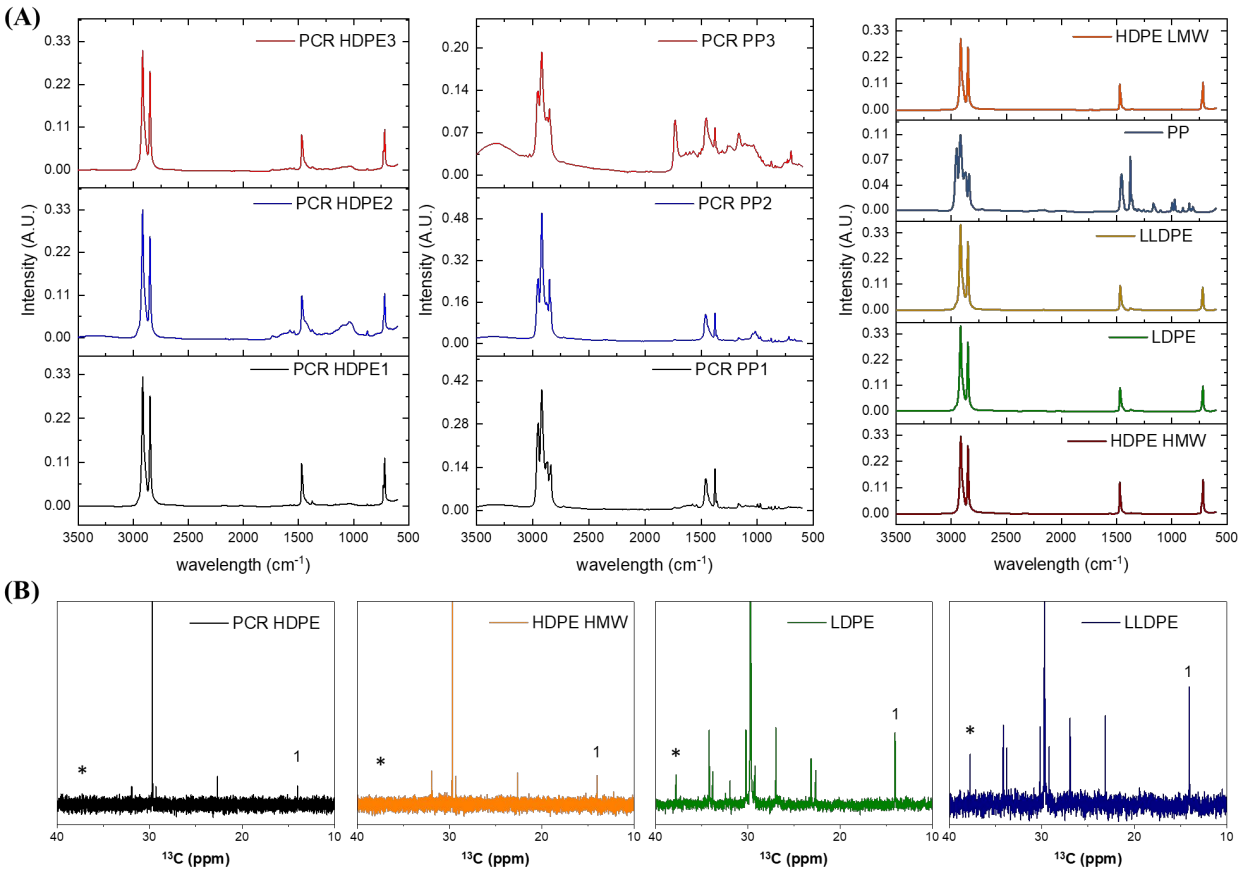

Fig.1. (A) ATR- FTIR spectrum of PCR HDPE, PCR PP and virgin polyolefins used in this study, (B) Zoomed in quantitative ^{13}C NMR results for PCR HDPE, HDPE HMW, LDPE, and LLDPE. The * sign is the tertiary carbon and 1 refers to the primary carbon which indicates the end groups.

3.2 Pyrolysis Results: Overall Product Yields and Feedstock Molecular Weight

Table 1 summarizes the molecular weight of the feedstock and the overall yields of the pyrolysis products. The light oil composition was in the naphtha range with a carbon distribution from C4 to C10. The heavy oil contained components larger than C10. All HDPE samples exhibited similar distributions, yielding around 24 wt% gas and 70 wt% oil, despite variations in their weight-average molecular weight (M_W) and number-average molecular weight (M_N). The solid yield of PCR HDPE was a little bit higher than the virgin HDPEs. LDPE had a lower oil yield and a higher total yield of gas and light oil than HDPE. LLDPE had a lower oil yield and a higher total yield of gas and light oil than LDPE. Thus, increasing the branch density in PE resulted in higher yields of light gases and light oils, while decreasing the yield of heavy oil, as depicted in Fig.2A. This result agreed with literature that branching reduces the plastic thermal stabilities because hydrogen on the tertiary carbons and tertiary carbon C-C bonds are more reactive than secondary carbons.[26, 27] Both PCR PP and virgin resin PP had the highest liquid yield (75 wt%) and the lowest gas yield (20 wt%), which is constant with the finding of Imtiaz et al.[28] The PP decomposition mechanism is likely different from PE as will be described in this paper.[16, 29, 30]

Table 1. Products distribution from polyolefins. The product distributions are all in wt%. The gas fraction included hydrogen and C1~ C3 hydrocarbons. The liquid fraction was the liquid product collected through the cold traps (C4 ~ C40+), and the solid fraction was the char formed during pyrolysis. The heavy oil fraction refers to compounds that have a boiling point higher than 175 °C (C10~C40+), and the light oil fraction refers to compounds that have a

boiling point lower than 175 °C (C4~C10). The normalized weights of the heavy and light oil fractions are shown in the parentheses.

	Manufacturer	M_W	M_N	Gas	Liquid	Solid	Heavy oil	Light oil	Mass Balance
HDPE HMW	Nova Surpass HPs167-AS	162920	27292	24.9 %	72.5 %	0.9 %	22.1% (31.5%)	50.4% (68.5%)	98.3 %
HDPE LMW	ExxonMobil Paxon AL55-003	93178	41937	24.4 %	70.9 %	1.7 %	18.4% (30.0%)	52.5% (70.0%)	97.0%
PCR HDPE	MRF collected PCR (ISU)	73963	36130	22.4 ± 1.2 %	69.8 ± 2.2 %	3.3 ± 0.8%	20.5% (29.4%)	49.3% (70.6%)	95.5 %
LDPE	LyondellBasell Petrothene NA216000	95064	26775	26.3 %	68.3 %	1.1 %	9.3% (13.6%)	58.9% (86.4%)	95.7 %
LLDPE	Exact 3040 Cast ExxonMobil	57369	41937	30.5 %	61.9 %	5.8 %	5.6% (9.1%)	56.3% (90.9%)	98.2%
PP	D218 Braskem	334060	138850	18.8 %	74.1 %	1.6 %	6.4% (8.7%)	67.6% (91.3%)	94.5%
PCR PP	MRF collected PCR (ISU)	188325	99299	20.7 %	76.2 %	0.4 %	16.2% (21.3%)	60.0% (78.7%)	97.3 %
The PCR HDPE pyrolysis was repeated 5 times									

The TGA results, presented in Fig.2B, demonstrated that all HDPE samples, despite the different molecular weight and sources, had similar degradation patterns in TGA. Most of the mass loss in all HDPE samples occurred between 450 °C and 520 °C, with the maximum mass loss rate observed at 495 °C. Both LDPE and LLDPE degraded between 420 °C and 510 °C, with the maximum mass loss rate at 485 °C. LDPE began degrading approximately 10 °C earlier than LLDPE, suggesting it may possess more thermal defects, such as methyl group branches, compared to LLDPE. These thermal defects will be further discussed in the subsequent DFT calculation section.

In contrast, PCR PP and PP, unlike HPDE samples, exhibited different degradation temperature zones even though they have similar products distributions as shown in Table 1. PCR PP experienced most of its mass loss between 360 °C and 485 °C, with the maximum mass loss rate at 460 °C, while virgin PP lost most of its mass between 380°C and 500 °C, with the maximum mass loss rate at 475 °C. Therefore, the TGA and DGT patterns cannot be used as the only source to predict the product distributions of the polyolefin pyrolysis.

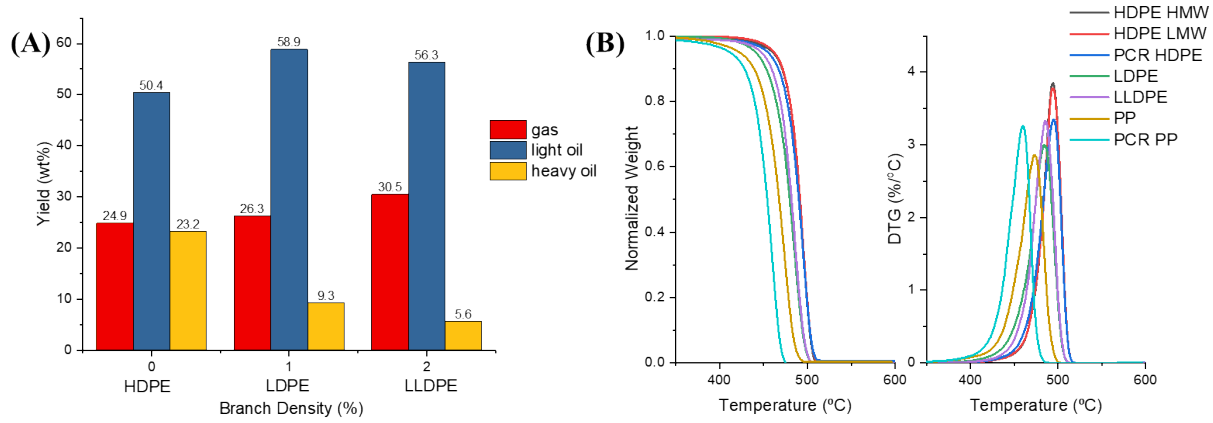

Fig.2. (A) The yield of gas, light oil, and heavy oils of HDPE (no branch), LDPE (1% of branch), and LLDPE (2% of branch) from Fluidized Bed Laboratory Pyrolysis Reactor. (B) Thermal decomposition of HDPE HMW, HDPE LMW, PCR HDPE, LDPE, LLDPE, PP, and PCR PP through TGA under N_2 condition (same particle size as feeding to the fluidized bed reactor).

3.3 Elemental Analysis of Plastics and Plastic Oils

Table 2 shows the metal analysis in the plastics and pyrolysis oils. The element mass balance was calculated from Eqn.1, which referred to the percentage of an element from the plastic that ended up in different fraction of oils. The sum element balance was calculated from Eqn.2, which referred to the percentage of the overall elements ended up in the different fraction of oils. We measured 14 elements: Mg, Al, Ca, Ti, Cr, Fe, Co, Ni, Cu, Zn, Cd, Sn, Sb, and Pb, as their derivatives are commonly used as catalysts, additives, fillers, or pigments in plastics. Trialkylaluminum ($Al_2(C_2H_5)_6$) and magnesium dichloride ($MgCl_2$) are co-catalyst and the support in Ziegler-Natta catalysts for polyolefin polymerization process.[31, 32] Common fillers and additives include calcium carbonate ($CaCO_3$), talc ($Mg_3Si_4O_{10}(OH)_2$), aluminum trihydroxide ($Al(OH)_3$), magnetite (Fe_3O_4), and stearates containing Ca, Mg and Zn.[32-34] Common inorganic pigments in plastics are titanium dioxide (TiO_2), zinc sulfide (ZnS), cadmium sulfide (CdS), chromium (III) oxide (Cr_2O_3), cobalt aluminate ($CoAl_2O_4$), and brass (Cu_3Zn_2).[35] Lead and nickel-based pigments were previously added to plastic products but now are limited due to regulatory restrictions for food or human contact products.[35] Elements Cu, Sn, and Sb were not detected in the sample plastics and their corresponding oils so they are not included in Table 2.

$$Element\ wt.\% = \frac{Concentration\ of\ the\ elements\ in\ oil \times wt.\%\ of\ the\ corresponding\ oil\ cut}{the\ amount\ of\ that\ element\ in\ the\ corresponding\ fed\ plastic} \quad \text{(Eqn.1)}$$

$$Sum\ wt.\% = \frac{\sum Concentration\ of\ the\ total\ elements\ in\ the\ oil \times wt.\%\ of\ the\ corresponding\ oil\ cut}{\sum Concentration\ of\ the\ total\ elements\ in\ corresponding\ fed\ plastic} \quad \text{(Eqn.2)}$$

PCR plastic samples had higher metal concentrations than virgin plastic resins. The virgin PE resins mainly contained Al (127 ~ 222 ppm), Ca (84 ~ 263 ppm), Co (39 ~ 764 ppm), and Zn (38 ~ 98 ppm), with trace amounts of Cr (5 ~ 24 ppm) and Fe (7 ~ 40 ppm). These elements could have been introduced through the use of $Al(OH)_3$ as a flame retardant, or $Al_2(C_2H_5)_6$ as a co-catalyst of Ziegler-Natta catalysts, calcium-zinc as a heat stabilizer, calcium stearate as a lubricant, and Cr as part of the PE synthesis Phillips catalyst.[33, 36] The PCR HDPE sample had higher metal content than virgin PE samples: with approximately double the Al content, 10-40 times higher Ca content, four times higher Cr content, and 3-15 times higher Fe content. The Co and Zn levels in PCR HDPE were similar to those in HDPE HMW. The virgin PP sample mainly contained Al (298 ppm), Ca (270 ppm), and Zn (56 ppm), with small amounts of Mg (56 ppm) and Fe (4

ppm). The PCR PP sample had similar amounts of Al, Mg, and Zn as PP but with much higher concentrations of Ca (4544 ppm), Fe (301 ppm) and Co (501 ppm). To summarize, PCR HDPE and PCR PP contained approximately 4400 ppm and 5800 ppm of trace metal elements, which was approximately 8 times and 24 times higher than their corresponding virgin resins, respectively.

After pyrolysis, most of the trace metals were lower in the pyrolysis oils compared to the corresponding feedstock materials. In PCR HDPE oils, the light oil only contained a total of 82 ppm metal, which was less than 1 wt% of the original metal content in the PCR HDPE. The heavy oil had a total of 157 ppm metal, also less than 1 wt% of the original metal content in the PCR HDPE. Therefore, more than 98 wt% of the total metal content was removed during PCR HDPE pyrolysis. In PCR PP oils, the light oil contained a total of 221 ppm of metals, and the heavy oil contained a total of 265 ppm of metals, representing 2.5 wt% and 0.8 wt% of the original metal content of PCR PP, respectively. Thus, over 96 wt% of the total metal content was removed for PCR PP. The metal concentrations in the plastic oils obtained from this study were lower than those reported in the literature for pyrolysis oil obtained without sand.[12] The sand thus likely acted as a getter during pyrolysis. The missing metal content probably was deposited on the sand and char which were not collected in this study.

The concentrations of the total minerals in the heavy oils were typically more than twice the concentration in the light oils for most of the plastics in this study (e.g., PCR HDPE light oil had a total metal concentration of 82 ppm, while PCR HDPE heavy oil had a total of 157 ppm). Thus, distillation could be used to further separate the inorganic fraction. This finding aligns with existing literature suggesting that distillation can effectively remove metal impurities from the oil.[37] However, in some cases (such as LDPE and LLDPE), the total metal concentrations in the plastic oils were comparable or even higher to those in the feed plastics. This is likely due to cross contamination due from previous experiments. In addition, as listed in Table 2, the mineral balances of Fe in several plastics were higher than 100 wt% and there were two potential reasons for this: 1) the cross contaminations and 2) the Fe leached from the stainless-steel fluidized bed reactor. The sand used in the fluidized bed reactor was replaced before PCR HDPE and PCR PP pyrolysis. When pyrolysis was conducted on fresh sand, as discussed before, most impurities were removed from the oil and likely ended up in the sand or char. More research is needed to better understand the buildup of inorganics on the sand.

Different elements had different removal efficiencies through the same pyrolysis process. Heavier elements (Co, Ni, Zn, and Pb) are more easily removed during pyrolysis with sand, while lighter elements (Al, Ca, and Fe) are more challenging to eliminate. For example, the Co concentration in HDPE HMW (764 ppm), PCR HDPE (906 ppm), and PCR PP (501 ppm) were high but no Co was observed in their pyrolysis oils. A similar trend was noted for Zn, with over 95 wt% of Zn removed from most plastics except for LDPE and LLDPE, which were likely cross-contaminated. In contrast, lighter elements such as Al, Ca, and Fe were present in most oils, with removal rates ranging from approximately 60 wt% to 80 wt%.

However, even though pyrolysis with sand and distillation could help remove the metal elements, the quality of the plastic oils still did not meet the requirements for the upgrading process. The most common method for upgrading the oil is feeding it into an industrial steam cracker.[8, 12, 29] Most oils did not meet the standards for Ca (0.5 ppm) and Fe (0.001 ppm), but did meet the standards of Ni (100 ppm) and Cu (50 ppm).[8] Further purification needs to be done to plastic pyrolysis oils before sending to steam cracker for upgrading.

Table 2. ICP analysis for plastic feedstock and pyrolysis plastic oils. LOD refers to the limit of detection, and LOQ refers to the limit of quantification. Trace element wt% calculation refers to the amount of a specific metal from the feed that is present in the light and heavy oils, as shown in Eqn 1. The calculation of sum wt% of the total elements in each oil is shown in Eqn 2. The abbreviation N.A. refers to not available, indicating that certain elements detected in the sample oils are not present in the corresponding plastic. This could be due to cross-contamination between experiments.

(ppm)	Sample/wt%	Mg	Al	Ca	Ti	Cr	Fe	Co	Ni	Zn	Cd	Pb	Sum
HDPE HMW	Plastic	60.70	186.22	262.68	<LOD	24.00	13.34	763.97	<LOD	98.06	<LOD	<LOQ	1408.97
	Light oil	<LOD	68.26	13.94	<LOD	<LOD	<LOQ	<LOD	<LOD	<LOD	<LOD	<LOQ	82.20
	wt%	*<LOD*	*18.47*	*2.67*	*<LOD*	*<LOD*	*<LOQ*	*<LOD*	*<LOD*	*<LOD*	*<LOD*	*<LOQ*	***2.94***
	Heavy oil	2.16	107.00	63.94	12.08	19.65	53.13	<LOD	<LOD	<LOQ	35.97	<LOQ	293.93
	wt%	*0.83*	*13.33*	*5.65*	*N.A.*	*19.00*	*88.02*	*<LOD*	*<LOD*	*<LOQ*	*N.A.*	*<LOQ*	***4.84***
HDPE LMW	Plastic	<LOD	127.76	60.32	<LOD	8.33	7.61	208.87	<LOD	68.27	<LOD	<LOQ	481.16
	Light oil	<LOD	126.63	31.42	<LOD	<LOD	1.66	<LOD	<LOD	<LOD	<LOD	<LOQ	159.71
	wt%	*<LOD*	*52.04*	*27.35*	*<LOD*	*<LOD*	*11.45*	*<LOD*	*<LOD*	*<LOD*	*<LOD*	*<LOQ*	***17.43***
	Heavy oil	2.52	131.23	74.23	17.5	21.46	64.28	<LOD	<LOD	<LOQ	4.24	<LOQ	315.46
	wt%	*N.A.*	*18.90*	*22.64*	*N.A.*	*47.40*	*155.42*	*<LOD*	*<LOD*	*<LOQ*	*N.A.*	*<LOQ*	***12.06***
PCR HDPE	Plastic	65.88	285.00	2205.49	97.38	84.17	252.14	905.72	<LOQ	97.44	124.56	251.33	4369.11
	Light oil	<LOD	63.36	16.92	<LOD	<LOD	<LOD	<LOD	<LOD	<LOD	<LOD	<LOQ	80.28
	wt%	*<LOD*	*10.96*	*0.38*	*<LOD*	*<LOD*	*<LOD*	*<LOD*	*<LOD*	*<LOD*	*<LOD*	*<LOQ*	***0.91***
	Heavy oil	<LOD	93.79	28.22	<LOD	<LOD	17.75	<LOD	<LOD	<LOQ	17.00	<LOQ	156.76
	wt%	*<LOD*	*6.75*	*0.26*	*<LOD*	*<LOD*	*1.44*	*<LOD*	*<LOD*	*<LOQ*	*2.80*	*<LOQ*	***0.74***
LDPE	Plastic	<LOD	130.46	58.12	<LOD	<LOQ	7.03	150.23	<LOD	38.60	<LOD	<LOQ	384.44
	Light oil	4.28	84.45	210.72	<LOD	<LOD	5.5	<LOD	<LOD	59.75	<LOD	<LOQ	364.70
	wt%	*N.A.*	*38.13*	*213.55*	*<LOD*	*<LOD*	*46.08*	*<LOD*	*<LOD*	*91.17*	*<LOD*	*<LOQ*	***55.88***
	Heavy oil	5.63	101.05	228.48	3.2	<LOQ	51.83	<LOD	<LOD	64.76	41.35	<LOQ	496.3
	wt%	*N.A.*	*7.20*	*36.56*	*N.A.*	*<LOQ*	*68.57*	*<LOD*	*<LOD*	*15.60*	*N.A.*	*<LOQ*	***12.00***
LLDPE	Plastic	<LOD	222.06	84.40	<LOD	<LOD	5.14	39.40	<LOD	53.35	<LOD	<LOQ	404.35
	Light oil	3.90	79.37	194.42	<LOD	<LOD	7.03	<LOD	<LOD	64.93	<LOD	<LOQ	349.65
	wt%	*N.A.*	*20.12*	*129.69*	*<LOD*	*<LOD*	*77.00*	*<LOD*	*<LOD*	*68.52*	*<LOD*	*<LOQ*	***48.68***
	Heavy oil	4.99	99.47	221.75	6.5	5.56	84.72	<LOD	<LOD	51.76	40.2	<LOQ	514.95
	wt%	*N.A.*	*2.51*	*14.71*	*N.A.*	*N.A.*	*92.30*	*<LOD*	*<LOD*	*5.43*	*N.A.*	*<LOQ*	***7.13***
PP	Plastic	56.23	297.28	270.41	<LOD	<LOD	3.78	<LOD	<LOQ	55.62	<LOD	<LOQ	683.32
	Light oil	<LOD	47.27	11.28	<LOD	<LOD	<LOD	<LOD	<LOD	<LOD	<LOD	<LOQ	58.55
	wt%	*<LOD*	*10.75*	*2.82*	*<LOD*	*<LOD*	*<LOD*	*<LOD*	*<LOD*	*<LOD*	*<LOD*	*<LOQ*	***5.79***
	Heavy oil	<LOQ	81.72	62.84	11.94	13.91	65.1	<LOD	5.88	2.31	2.23	<LOQ	245.93
	wt%	*<LOQ*	*1.76*	*1.49*	*N.A.*	*N.A.*	*110.22*	*<LOD*	*N.A.*	*0.27*	*N.A.*	*<LOQ*	***2.30***
PCR PP	Plastic	160.90	191.30	4543.67	31.992	4.45	300.61	500.87	41.92	17.05	<LOQ	<LOQ	5792.76
	Light oil	19.29	138.01	60.48	<LOD	<LOD	2.92	<LOQ	<LOD	<LOQ	<LOD	<LOD	220.70
	wt%	*7.19*	*43.29*	*0.80*	*<LOD*	*<LOD*	*0.58*	*<LOQ*	*<LOD*	*<LOD*	*<LOD*	*<LOD*	***2.29***
	Heavy oil	19.53	173.00	65.77	<LOQ	<LOQ	4.14	<LOQ	<LOD	2.77	<LOD	<LOD	265.21
	wt%	*1.97*	*14.65*	*0.23*	*<LOQ*	*<LOQ*	*0.22*	*<LOQ*	*<LOD*	*2.63*	*<LOD*	*<LOD*	***0.74***
LOD		1.03	6.43	0.13	0.47	1.40	0.37	0.93	1.23	0.53	0.10	3.97	
LOQ		3.44	21.44	0.44	1.56	4.67	1.22	3.11	4.11	1.78	0.33	13.22	

3.4 Detailed Hydrocarbon Composition Analysis

The GC×GC-FID chromatograms of all 7 types of plastics pyrolysis oils at 500°C are depicted in Fig.3. GC×GC-FID enabled effective separation of compounds within the carbon number range of C4 to C40, identifying over 1000 peaks for each oil. In a GC×GC chromatogram, a complex mixture is separated based on boiling points on the x-axis (retention time for the first column) and functionality on the y-axis (retention time for the second column). Along the x-axis, the boiling points of the compounds increase from left to right. Along the y-axis, the polarity of the compounds increases from top to bottom. These peaks were categorized into 6 groups: linear hydrocarbons, branched alkanes, branched alkenes, branched alkadienes, aromatics, and dicyclo-aromatics (aromatic compounds with multiple rings). The template of the GC×GC-FID is provided in ESI Fig.S4. The linear hydrocarbons were further divided into linear alkanes, alkenes, and alkadienes using another GC, with the detailed procedure provided in the ESI. According to the GC×GC chromatograms, compared to PE oils, PP oils contained more aromatics and less alkenes. The plasticizer, bis(2-ethylhexyl) terephthalate, was detected in all plastic oils. The quantification results from GC×GC-FID were validated through detailed hydrocarbon analysis (DHA) and nitric oxide ionization spectroscopy evaluation (NOISE) results, as shown in ESI Fig.S5.

The gas products from the pyrolysis of all seven types of plastic were quantified using a refinery gas GC (RGA). A detailed analysis of the gas products is provided in ESI Fig. S6. The gas compositions of PP and PE resins differed. The gas products generated from PE pyrolysis were similar (Fig. S6 A~E); the major components, ranked in order of abundance from highest to lowest, were ethylene, propylene, ethane, and methane. For the gas products generated from PP pyrolysis (Fig. S6 F&G), the major components, ranked in order of abundance from highest to lowest, were propylene, ethane, ethylene, methane, and propane. Additionally, PP generated less hydrogen compared to PE. In the gas phase, ethylene had the highest yield among all PE plastics, while propylene had the highest yield in PP plastics. This indicated that β-scission was occurring. However, the overall yields of both ethylene and propylene were below 10 wt%, suggesting that β-scission is not the dominant reaction in polyolefin pyrolysis.

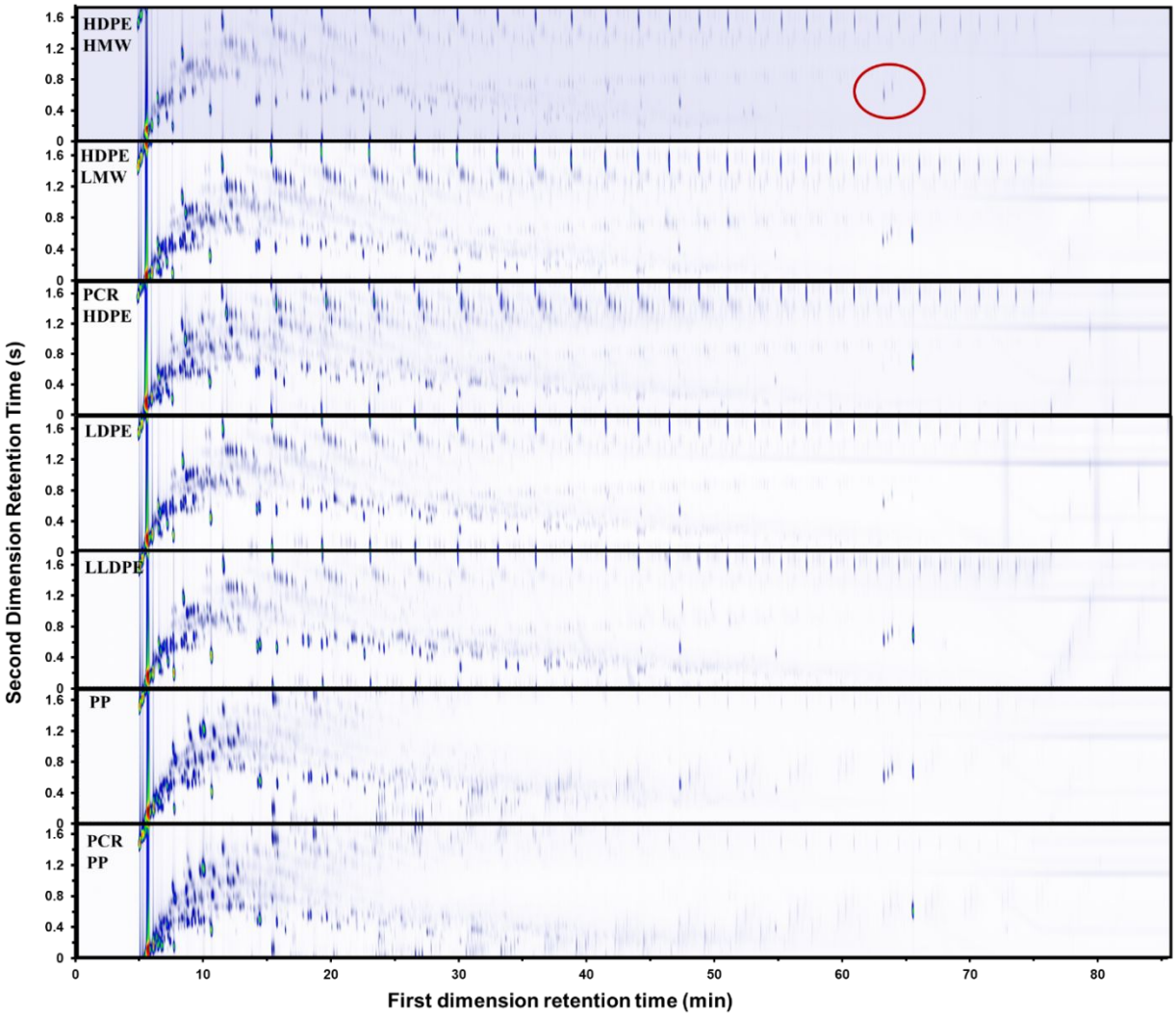

Fig.3. GC×GC-FID chromatographs of HDPE with high weighted molecular weight, HDPE with low weighted molecular weight, PCR HDPE, LDPE, LLDPE, PP, and PCR PP. The circled component is Bis(2-ethylhexyl) terephthalate, a common plastic additive.

The major products in the polyolefin oils generated in this study are alkanes, alkenes, alkadienes, and mono-aromatics. Although some dicyclo-aromatics were detected, their yields were below 5 wt% in all oils. The quantities of these compounds varied among different polyolefins. Fig.4A showed the quantified compositions of the oils. HDPE HMW, HDPE LMW, and LDPE had similar distributions: approximately 30 wt% alkanes, 40 wt% alkenes, 15 wt% alkadienes, and 10 wt% mono-aromatics. PCR HDPE contained around 10 wt% fewer alkanes and 5 wt% more alkenes compared to virgin HDPE. LLDPE oil had a similar alkane content to HDPE oils but a lower alkene yield (30 wt%) and a higher aromatic yield (25 wt%). PCR PP and PP oils had the highest alkane yield (40 wt%) and the lowest alkene yield (25 wt%) among all seven plastics. Additionally, PCR PP contained about 5 wt% more alkadienes than virgin PP.

Fig.4B shows the composition of the light oil (C4-C10). Fig.4C shows the composition of the heavy oil (C11-C40). Generally, light oils had similar yields of alkanes, alkenes, and aromatics but contained more alkadienes compared to the whole oil. In the heavy oils, branched structures were distinguishable by GC×GC and were labeled as iso-alkane, iso-alkene, and iso-alkadiene Fig.4C. Both PCR HDPE and PCR PP had higher concentrations of branched compounds. PCR HDPE contained 15 to 25 wt% higher content of the branch alkene and 5% higher content of alkadienes than HPDE resins. PCR PP contained 5 wt%

more brancedh alkanes and alkadienes, and around 10 wt% more branched alkenes than the PP resin. In addition, as the branch density in the polyolefin increased, the yield of dicyclo-aromatics in the heavy oil also increased. Although LLDPE, PP, and PCR PP contained 30 ~ 40 wt% of the dicyclo-aromatics, the yield of the heavy oil was less than 10 wt% (Table 1), resulting in low total yields.

Alkanes, alkenes, and alkyl radicals are initially formed during the decomposition of PEs. As the alkenes continue to degrade, more alkanes and alkadienes can form.[4] Consequently, with an increase in secondary reactions, more alkanes, alkadienes, and aromatics will be generated.[4] Comparing the pyrolysis results between HDPE HMW and LMW (Fig.4B), HDPE LMW exhibited higher yields of alkanes and alkadienes in the C4-C10 range. This suggests that during pyrolysis, lower molecular weight polymers are less thermally stable than higher molecular weight polymers and undergo more secondary reactions, despite showing similar degradation patterns in TGA (Fig.2B).

Increasing branch density decreases the thermal stability of the polymer because it introduces more reactive tertiary hydrogens and weaker carbon-to-carbon bonds on the tertiary or quaternary carbon atoms.[26, 38] This trend was evidenced not only by the liquid yield but also the detailed products distribution. In the pyrolysis results of HDPE HMW, LDPE, LLDPE, and PP, an increase in branch density led to a decrease in alkenes yield and an increase in the yield of alkane, and a total yield of alkadiene,aromatics, and dicyclo-aromatics, as alkenes decompose into alkanes and alkadienes, and alkadienes further form aromatics. Aromatics then can further convert to dicyclo-aromatics due to the addition of small alkene molecules like ethene.[39]

When comparing the pyrolysis results of PCR plastics to their corresponding virgin resins, it appears that the impurities or additives in PCR plastics served two roles: promoting hydrocarbon isomerization and preventing hydrocarbon oligomers decomposition This was evidenced by Fig.4A and Fig.4C, which showed that PCR HDPE had the highest yields of branched alkanes, alkenes, and alkadienes, as well as an overall higher alkene yield, indicating fewer secondary reactions. PCR PP oils contained a higher concentration of branched compounds but relatively similar alkenes concentration. Further investigation is needed to determine the specific impurities responsible for hydrocarbon isomerization during pyrolysis.

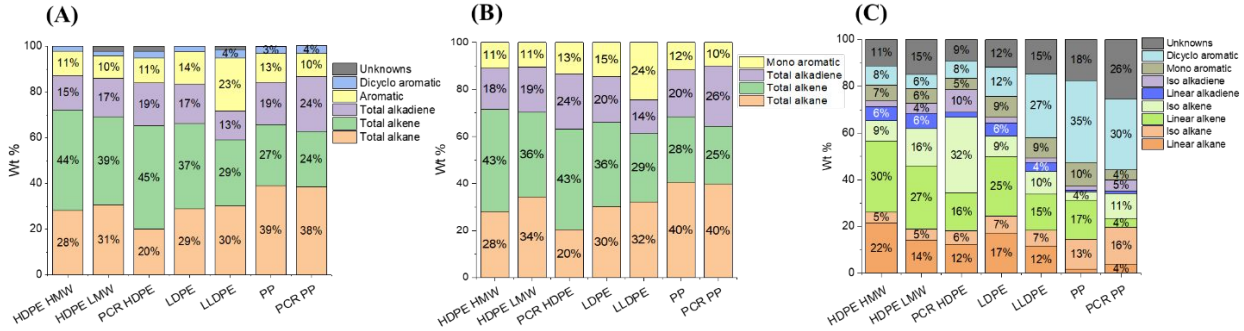

Fig.4. The overall summary of oil weight percent distributions of (A) whole oil, (B) light oil, and (C) heavy oil with branch analysis for all 7 plastic pyrolysis oils, quantified through GC×GC-FID.

Alkenes are one of the most abundant products in pyrolysis oils, and their structures were further studied using NMR. Fig.5 presented the alkene composition normalized by total alkenes. Examples of ^{1}H NMR spectra for the light and heavy oils of PCR HDPE and PCR PP were shown in ESI Fig.S7. Three main types of alkenes were detected in both oils: terminal alkenes, internal alkenes, and 1,1-disubstitued alkenes. The conjugated alkadienes and cyclic alkenes (e.g. compound with structures like cyclohexene) were only detected in light oils in this study through ^{1}H NMR, which aligns with the findings of the Abbas-Abadi et al. and Krishna et al.'s studies that conjugated alkadienes and cyclic alkenes were only existing in small molecules.[13, 15] The formation of cyclic olefins and conjugated alkadienes might result from secondary

reactions, as the compounds in the heavy oil underwent fewer cracking reactions. This phenomenon emphasized the significant impact of secondary reactions on the formation of different groups of pyrolysis products.

Terminal alkenes were the most abundant, comprising approximately 50-60 mol% of the light oil among all PE samples. Internal alkenes were around 15-25 mol%. Less than 10 mol% of the products were 1,1-disubstituted alkenes, cyclic alkenes, and conjugated dienes, respectively. In heavy PE oils, terminal alkenes remained the most abundant, but the proportion of 1,1-disubstituted alkenes dropped to less than 5 mol%. In light PE oils, the amount of internal alkenes increased with higher branch density, while the amount of cyclic alkenes and conjugated alkadienes remained relatively similar. In heavy PE oils, the proportions of internal and terminal alkenes were comparable. In light PP oils, 1,1-disubstituded alkenes were the most abundant products (60 mol%) and contained approximately 20 mol% of terminal alkenes and 15 mol% of internal alkenes. In heavy PP oils, the amount of the internal alkenes increased to 30 mol% and the 1,1-disubstitued alkenes decreased to 45 mol%.

Overall, light oils contained more 1,1-disubstituted alkenes, cyclic alkenes, and conjugated dienes than heavy oils across all samples. The main difference between PE and PP oils was the different concentrations of in the1,1-disubstituted alkenes. For PE oils, the higher concentration of 1,1-disubstituted alkenes in light oils compared to heavy oils likely resulted from secondary pyrolysis reactions. In contrast, 1,1-disubstituted alkenes in PP oils likely formed during the primary degradation reaction, making them predominant in both PP heavy and light oils, as further discussed in Sections 3.6 and 4.1. However, PP heavy oils showed a noticeable increase in internal alkenes compared to light oils. This might be due to NMR's limitation in distinguishing specific molecules. Hence, it is possible that in PP heavy oil, some dicyclo-aromatics (as it was one of the main compounds in PP heavy oil revealed by GC×GC) with side chains containing internal alkenes were present.

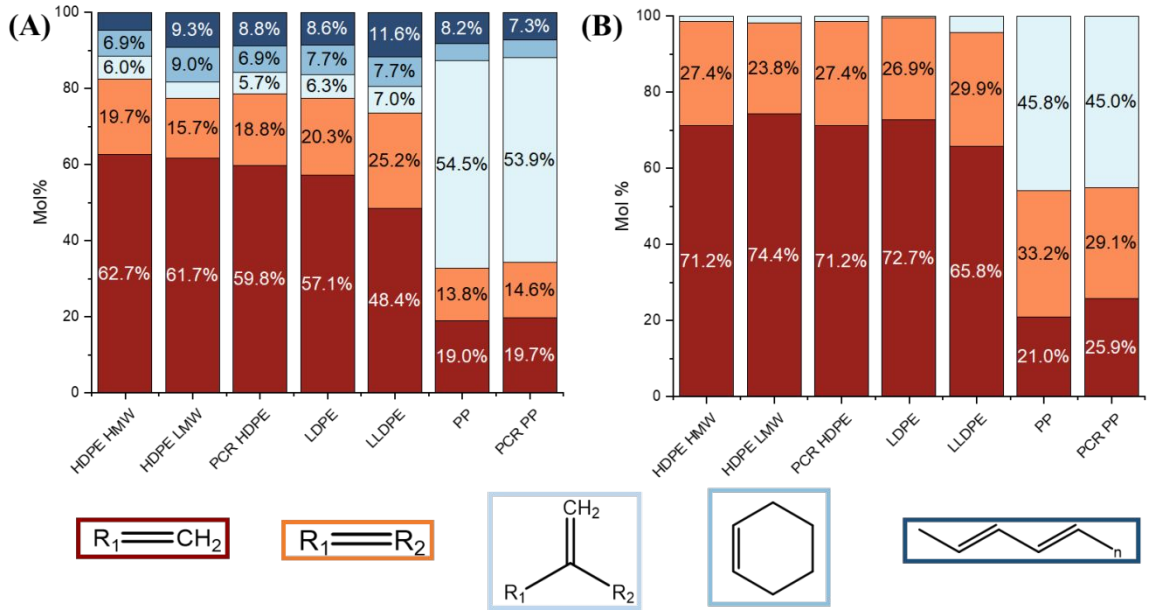

Fig.5. Normalized molar percentage of terminal (crimson), internal (orange), and 1,1- disubstituted (light blue), and cyclic (mid-blue) alkenes, as well as conjugated dienes (navy blue) quantified through 1H NMR for (A) light oils and (B) heavy oils.

Fig.6 illustrated the quantified results for each group of compounds distributed by carbon number. Among all HDPE oils, even though they had relatively similar gas, liquid, and solid yields (Table 1) and TGA patterns (Fig.2B), their carbon distributions were different. For HDPE samples, HDPE HMW had the highest molecular weight, followed by HDPE LMW and PCR HDPE. HDPE LMW exhibited the sharpest

distribution, resulting in the highest C5 and C6 yields among HDPE samples. PCR HDPE and HDPE HMW oils had similar carbon distributions, despite HDPE HMW's molecular weight being more than double that of PCR HDPE. This similarity in carbon distribution may be attributed to certain additives in PCR HDPE that could inhibit oligomer degradation. Fig.S8 in the ESI provided branching information from C7-C40. According to Fig. S8, HDPE HMW has the highest yields of linear alkanes and alkenes, while PCR HDPE has the highest yields of branched alkanes and alkenes.

Comparing HDPE LMW, LDPE, and LLDPE highlighted the impact of PE structure on plastic oils' product distributions. In Fig.6, LDPE had a similar product carbon distribution to HDPE LMW but with higher benzene and toluene yields. LLDPE pyrolysis products showed different carbon distributions from both LDPE and HDPE LMW with a higher C1 to C3 yield and lower C4 to C6 yield. LLDPE also had the highest yields of ethene and aromatics (Fig. S8E shows LLDPE aromatic yields close to 50% from C7-C40). These results further suggested that branching in PE promotes thermal degradation.

The PP carbon distributions differed from those of PE samples, exhibiting much sharper distributions, with a 25 wt% of C5 yields. In PE samples, C2 (ethane and ethene) always had a higher or similar yield to C3 (propane and propene). This indicated that PP degradation was dominated by "unzipping reactions" since propene is the monomer of PP. In contrast PE degradation was dominated by random scission reactions. PP oils also had the lowest benzene yield and tended to have more branched aromatics (toluene and xylenes) and more branched alkanes and alkenes (ESI Fig.S8).

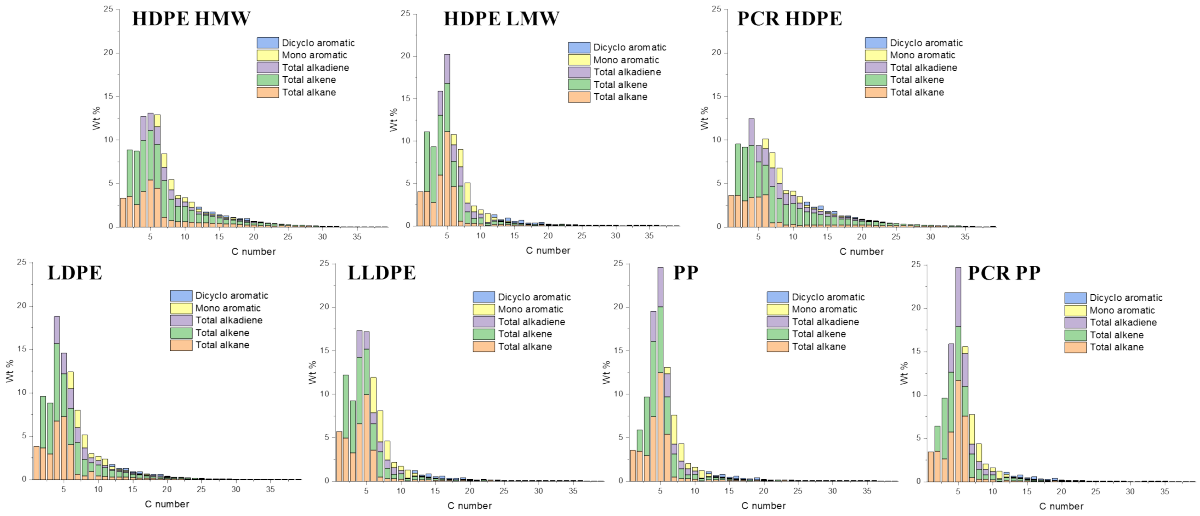

Fig.6. The detailed product analysis with each carbon number of HDPE HMW, HDPE LMW, PCR HDPE, LDPE, LLDPE, PP, and PCR PP, the total amounts of C3 and C4 products were modified by the solubility of propane and butane in hexane at room temperature.[40, 41]

3.5 Schultz-Flory Distributions of Polyolefin Pyrolysis Oils

Schultz-Flory distribution model[42-44] was applied to the products from all 7 types of plastic oils. The model is described as Eqn. 3. Where C_n is the carbon selectivity of the alkane and alkene of each carbon number as they are the main primary products from pyrolysis, n is the carbon number, α is originally the chain-growth probability, and (1- α) is the termination probability for the polymerization. When a polymer degradation process follows random scission reactions, the products tend to form a Schultz-Flory distribution. This hypothesis has been applied to polyolefin thermal degradations.[45, 46] In this context, α in Eqn.2 represents the likellihood of the polyolefin following random scission reactions.

$$Ln\left(\frac{C_n}{n}\right) = (n-1)\ln(\alpha) + 2\ln(1-\alpha) \quad \text{(Eqn. 3)}$$

Not all polyolefins thermal degradation products conformed to the Schultz-Flory distribution. As shown in Fig.7A, all HDPE samples fitted the Schultz-Flory distribution, with α values ranging from 0.72 to 0.75 and R^2 values above 0.9. With the increasing of the branch density of polyolefins, both α and R^2 values decrease (Fig.7B). The α value of LDPE decreased to 0.715, with an R^2 of 0.904, still indicating a reasonable fit. However, LLDPE had a similar α value to LDPE but the R^2 went down to 0.633, which was off from the fitting. In Fig.7C, the α value of PP further decreased to 0.645 with an R^2 of 0.360, suggesting that PP degradation products did not follow the Schultz-Flory distribution. A similar pattern was observed in the PCR PP.

Therefore, the HDPE samples pyrolyzed in this study followed random scission reactions, which was consistent with other literature reports.[17, 47] As the branch density in the plastics increased, the likelihood of plastic underwent random scission reaction decreased, which was indicated by the lack of fitting of LLDPE, PP, and PCR PP product distribution to the Schultz-Flory distribution. This finding indicated that increased branching affected the degradation pattern and chemistry of polyolefins. Further discussion is in Section 4.1.

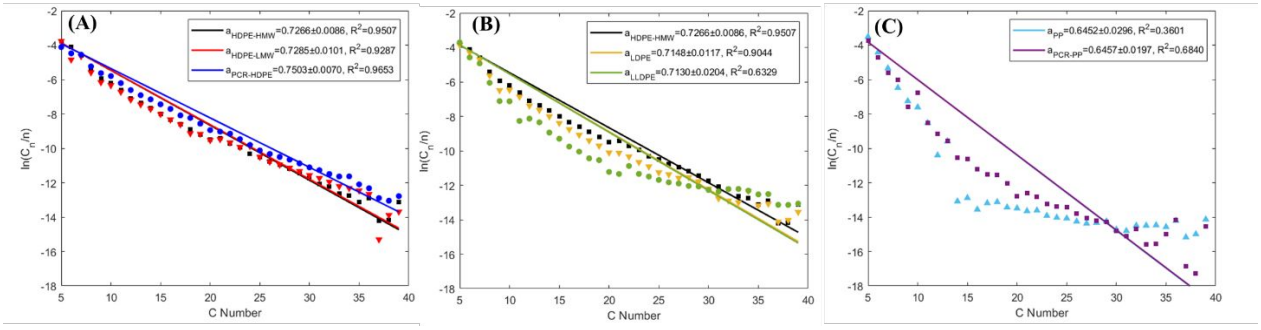

Fig.7. Schultz-Flory distribution plots for products (C5+) with (A) all HDPE samples, (B) all virgin polyethylene resins, and (C) all PP samples. The α values include a 95% confidence interval.

3.6 DFT Calculations

ab initio calculations of the thermochemistry and kinetics of HDPE, LLDPE, and PP pyrolysis were conducted by varying branch size, density, and position in the linear C10 backbone (Fig.8A) to reveal the branches' effects on product selectivity towards light oil and gas products. Fig.8B shows the DFT-derived activation energy barriers for C-C scission in HDPE, PP, and LLDPE. The backbone C-C scission in HDPE (blue bar) requires an activation energy barrier of 365.4 kJ/mol, which is higher than that for PP (321.3 kJ/mol, purple bar) and LLDPE (315.3 kJ/mol, red bar). Such a significant barrier reduction from HDPE to LLDPE indicates that branching can promote the backbone C-C cleavage. Therefore, a higher amount of backbone C-C scission is expected in the hydrocarbon polymers with branches, which can also qualitatively explain our experimental observation that LLDPE and PP yield more light oil products than heavy oil products (Fig.2A). Further, our computational chemistry findings suggest that the amount of light oil from the branched polymers (LLDPE and PP) is higher than that from the non-branched one (HDPE), which agrees with our experimental findings (Fig.2A). Importantly, we determined that the activation energy for the backbone C-C scission in LLDPE is lower than that for PP (Fig.8B), which suggests that larger branch sizes and lower branch density facilitate easier backbone C-C scission. This may be due to the highest occupied molecular orbital (HOMO) electrons accumulating in the middle C-C sites of LLDPE for backbone scission (Fig.8C).

To further investigate the role of branch size on the pyrolysis product selectivity, we calculated the barrier of the backbone C-C scission in LLDPE by varying the branch length from methyl to ethyl, propyl, butyl, pentyl and hexyl (ESI Fig.S10). A notable effect of branch size was not observed when going from methyl to ethyl, facilitating the kinetics of C-C scission. Meanwhile, we observed that if the branch is a methyl group, the polymer backbone tends to break first; if the branch is longer than a methyl group (>1 carbon), the whole branch tends to be cleaved off from the backbone first. Therefore, the butyl as branch (corresponding to LLDPE) contributes to the lower energy cost of the C-C scission in the branch than in the backbone, which leads to the highest selectivity towards gas in LLDPE pyrolysis (Table 1). In contrast, the lower methane selectivity (one of the major gas components) (Fig.6) of PP pyrolysis can be explained by the lower priority of methyl branch broken than the backbone C-C scission. The limited gas selectivity of PP pyrolysis can also be understood by the energy profiles of the most favorable pathways for the gasification of our HDPE and PP models (ESI Fig.S11). Through DFT calculations, we found the presence of methyl branch increases carbon number of ultimate products, which in turn indicates the incomplete gasification and favors liquid production. Therefore, the significant role of branch length on the backbone and branch C-C scission in HDPE, PP and LLDPE can reveal the intrinsic reason for product selectivity towards liquid and gas product distributions of the three polymers as observed in our experiments.

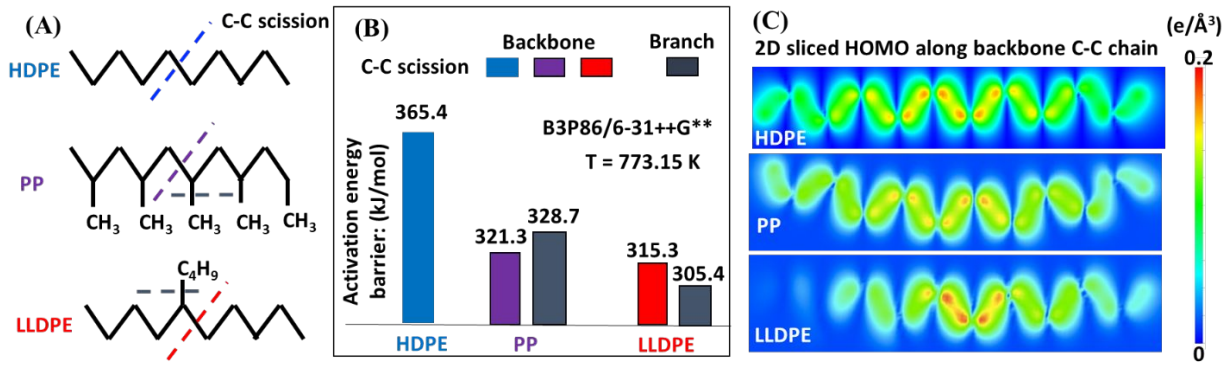

Fig.8. (A) Schematics of the initial configurations of model compounds of HDPE, LLDPE and PP, in which the dashed line refers to the backbone and branch C-C scission sites. (B) The calculated activation energy barriers for backbone C-C scission in HDPE (blue bar), PP (purple bar), LLDPE (red bar), and branch C-C scission in PP and LLDPE (grey bars). (C) The two-dimensional (2D) sliced highest occupied molecular orbital (HOMO) electron density of HDPE, LLDPE and PP along the backbone C-C chains.

4. Discussion:

4.1 The Impact of Polymers' Structures

The polymer branch structure impacts the distribution of gas, liquid, and solid products (Table 1) due to its effect on thermal stability and degradation kinetics.[26] This is supported by DFT calculations, which show that PP requires about 44 kJ/mol less energy than other polymers for C-C bond cleavage. LLDPE requires about 60 kJ/mol less energy at thermal defects to initiate degradation compared to the HDPE (Fig.8B). The polymer contains more thermal defects as the branch structure increases leading to a faster decomposition rate and resulting in more secondary reactions. Consequently, these polymers' pyrolysis oils contain less alkenes, higher alkanes, alkadienes, and aromatics (Fig.4).

Branching structure also produces more internal olefins. For LLDPE, there are two possible pathways to initiate degradation as depicted in Fig.9A: cleavage from the side chain or from the backbone. Regardless of the cleavage points, the presence of branches in LLDPE increases the likelihood of forming internal radicals without isomerization. The combination of DFT (Fig.8B) and NMR (Fig.5A) results suggest that LLDPE degradation likely begins with side chain cleavage, forming a short-chain paraffin with a long internal radical. This internal radical can then undergo β-scission, resulting in the formation of a relatively short-chain internal alkene.[47, 48] This is further supported by Fig.6, which shows that LLDPE has

a higher C4 yields compared to HDPE (the LLDPE used in this study is a copolymer of ethene and hexene, so it contained C4 length of side chain). Although the LDPE has a higher yield of C4 when compared to LLDPE, predicting the composition of LDPE decomposition is more challenging due to its unknown branch structures of LDPE.

As shown in Fig.5A, LLDPE oils exhibit 10 mol% more internal alkenes than HDPE oils, despite having only 2% branch content in the original polymer. This may be caused by the double bond isomerization of alkenes at high temperature. According to our previous study,[10] internal alkenes are more thermodynamically favored to form compared to terminal alkenes. Since the LLDPE requires a lower degradation energy (Fig.8B) more secondary reactions including double bond isomerization would have a higher chance to take place during the pyrolysis and therefore has a higher yield of internal alkenes.

Fig.9B illustrates the plausible initiation pathways for PP thermal degradation. According to the DFT calculation (Fig.8B) and NMR data (Fig.5), PP primarily degrades through the carbon backbone, forming a 1,1-disubstituted alkene and an alkane. Some literature suggests that PP degradation involves random scission followed by an unzipping process.[49-51] Once the initial backbone C-C scission occurs (random scission), the generated radicals initiate the unzipping process. This is further supported by Fig.6, where among all polyolefin pyrolyzed under the same condition, PP and PCR PP have the lowest yields of methane, indicating the unfavored cleavage from the methyl branch, as supported by the DFT calculation (Fig.8B). Additionally, the high methyl branch content in PP favors the oil yields (Fig.S11), which explains why PP has the highest oil yield among all polyolefins. Additionally, PP heavy oils exhibit a higher concentration of dicyclo-aromatics, likely due to the methyl branches facilitating the cyclization of PP oligomers, consistent with observations from other studies.[14]

Furthermore, the Shultz-Flory plot (Fig.7B) indicates that higher branch density in polyolefins reduces the likelihood ofrandom scission during pyrolysis. For PE samples, the HDPE samples have undetectable tertiary carbons (Fig.1B), indicating minimal thermal defects, and thus the carbon backbone decomposes at randomly distributed C-C bonds. For high branch density PE samples, such as LLDPE, the branches cleave first from the carbon backbone, and the generated internal radicals may deviate the polymer degradation process from the random scission pathway. In PP samples, degradation begins with random scission followed by an unzipping reaction, which resulted in the poor fit to the Schultz-Flory distribution.

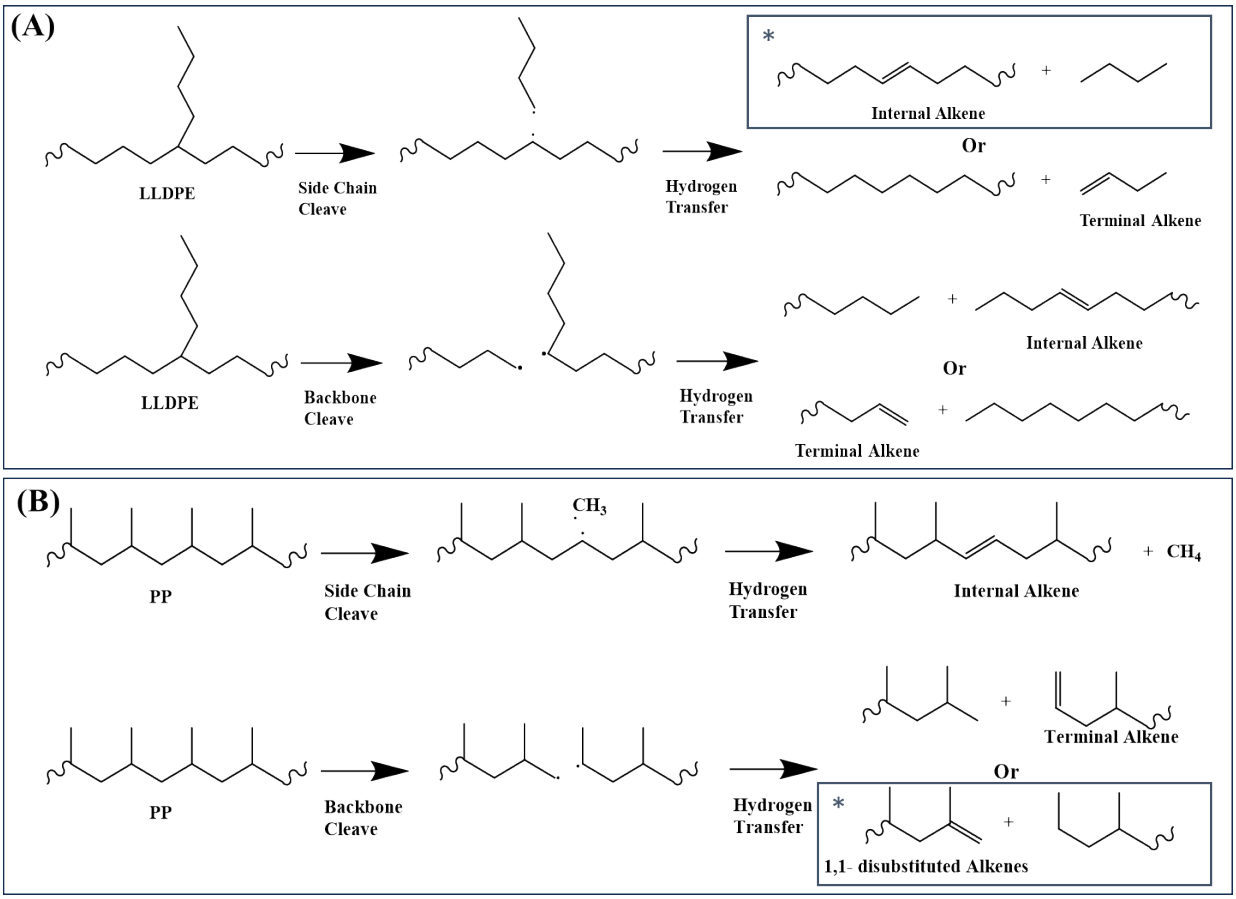

Fig.9. The plausible (A) LLDPE and (B) PP thermal degradation pathways. The star sign indicates the most favored degradation pathway.

4.2 The Impact of Polymers' Molecular Weight

In this study, molecular weight (MW) did not significantly affect the gas, liquid, and char distribution for HDPE samples (Table 1). However, lower MW led to a higher yield of C4-C10 compounds and higher yields of paraffins and aromatics in the overall oil (Fig.4 and Fig.6). This may be attributed to the relatively mild pyrolysis temperature and long residence time used in this study. At 500 °C, hydrocarbons with carbon numbers less than or equal to C10 barely degrade.[10] At this temperature, smaller molecules (C4-C10) barely decompose to non-condensable molecules (C1-C3), leading to similar gas yields among all HDPE samples. The relatively long residence time allows for more secondary reactions for small MW polymer to take place, leading to higher concentrations of alkanes and alkadienes. In addition, the two PP samples, despite having higher molecular weight than PE samples, showed much sharper and lighter product distributions (Table 1 and Fig.6). This result further supports the hypothesis that polymer structure has a greater impact on pyrolysis product distribution than molecular weight.

4.3 The Impact of Polymers' Sources

The impact of additives in PCR plastics is complex, and the additives content in PCR plastics can vary significantly from batch to batch. According to Fig.4C, Fig.6, and ESI Fig.S8, PCR plastics produce more branch products during pyrolysis. Acid catalysts, such as $AlCl_3$, are well-known for promoting alkane skeletal rearrangement reactions to form branched alkanes.[52] The branched alkenes may resulted from the decomposition of the long chain alkanes. Although the Al concentration in PCR plastics is not significantly

different from that in virgin resins (Table 2), other impurities in PCR plastics might create an acidic environment and synergize with Al to catalyze hydrocarbon isomerization.

Unlike Al, Ca is detected as one of the main impurities in PCR plastics, originating from fillers, stabilizers, and lubricants.[33, 36, 53] CaO, which forms from the decomposition of the common Ca additive $CaCO_3$, can act as a catalyst for the isomerization and hydrogenation of alkene.[54] However, the concentrations of internal alkenes (Fig.5) and alkanes (Fig.4A~C) in the PCR plastic oils were not higher than the corresponding virgin resins. There are two possible explanations for this: first, the pyrolysis temperature is too low for $CaCO_3$ to degrade into CaO; second, the limited hydrogen generation during pyrolysis may slow the hydrogenation rate of alkenes. Other forms of Ca, such as Ca salts, can serve as heat stabilizers in PE (which may also be Zn or Pd salts).[8] These heat stabilizers may reduce the thermal degradation rate of PE. Therefore, PCR HDPE shows more C10+ products and a broader product distribution compared to virgin HDPE resins (Fig.3A). PP usually does not contain stabilizers.[53] Although the PCR PP also has a slightly wider distribution of the products, it is not as significant as the PCR HDPE.

Despite the changes in the oil compositions, the main challenge in pyrolyzing PCR plastics remains the removal of impurities from the plastic oils and managing the carryover of impurities from different plastic sources (Table 2). While pyrolysis with distillation process can remove 80 ~ 90 wt% of the metal contents, the issue of impurity removal persists.

5. Conclusions:

Seven types of virgin and PCR plastics, including PCR HDPE, PCR PP, and virgin resins with varying molecular weights of HDPE, LDPE, LLDPE, and PP, were pyrolyzed in a fluidized bed reactor. Polymer structure had the greatest influence on pyrolysis product distributions, while molecular weight had the least impact. The predominant compounds found in the pyrolysis oils were alkane, alkene, alkadiene, aromatic, and dicyclo-aromatics, with variations in composition observed across different plastic feedstocks. HDPE oils had relatively higher yields of alkenes and alkadienes and lower yields of alkanes. In contrast, LLDPE oils showed lower yields of alkenes and alkadienes but higher yields of alkanes and aromatics compared to HDPE oils, PP oils had even lower yields of alkenes and alkadienes with higher yields of alkanes and aromatics. This is because branches in polyolefins are usually identified as thermal defects where polymer degradation initiates; therefore, with more branch structures, more secondary reactions occur, resulting in a lower yield of alkenes.

DFT calculations also revealed that, in the absence of branches or with a methyl group branch, the cleavage of the polymer C-C backbone required 365.4 kJ/mol and 321.3 kJ/mol for HDPE and PP respectively. Conversely, in polymers like LDPE and LLDPE, where branches contain more than one carbon, branch cleavage from the backbone occurred first, requiring lower energy (305.4 kJ/mol) forming internal olefins. Higher branch density in PE resulted in increased concentrations of aromatics, branched and non-branched alkanes due to more frequent secondary reactions.

Pyrolysis oil derived from PCR HDPE and PCR PP contained a higher proportion of branched compounds compared to virgin plastics. Additives, such as trace elements present in PCR plastics, could potentially promote the isomerization of linear hydrocarbons to branched forms during pyrolysis. While pyrolysis effectively eliminated most trace elements, additional purification steps may be necessary for the resultant oils.

6. Data Availability Statement

The data supporting the results of this study are included within the manuscript and in the supplementary information (ESI). For any further data requests, please reach out to the corresponding author. Your inquiry will be promptly addressed to enhance the understanding of the research.

7. Acknowledgement:

This material is based upon work supported by the U.S. Department of Energy, Office of Energy Efficiency and Renewable Energy, Bioenergy Technologies Office under Award Number DEEE0009285.

References:

1. M. Garside, *Global plastic production 1950-2022*, Statista, 2024.
2. R. Geyer, J. R. Jambeck and K. L. Law, *Science Advances*, 2017, **3**, e1700782.
3. *Advancing Sustainable Materials Management: 2018 Tables and Figures* United States Enviornmental Protection Angency, 2020.
4. H. Li, H. A. Aguirre-Villegas, R. D. Allen, X. Bai, C. H. Benson, G. T. Beckham, S. L. Bradshaw, J. L. Brown, R. C. Brown, V. S. Cecon, J. B. Curley, G. W. Curtzwiler, S. Dong, S. Gaddameedi, J. E. García, I. Hermans, M. S. Kim, J. Ma, L. O. Mark, M. Mavrikakis, O. O. Olafasakin, T. A. Osswald, K. G. Papanikolaou, H. Radhakrishnan, M. A. Sanchez Castillo, K. L. Sánchez-Rivera, K. N. Tumu, R. C. Van Legn, K. L. Vorst, M. M. Wright, J. Wu, V. M. Zavala, P. Zhou and G. W. Huber, *Green Chemistry*, 2022, **24**, 8899-9002.
5. D. I. W. Posch, in *Applied Plastics Engineering Handbook (Second Edition)*, ed. M. Kutz, William Andrew Publishing, 2017, DOI: https://doi.org/10.1016/B978-0-323-39040-8.00002-X, pp. 27-53.
6. K. Ragaert, L. Delva and K. Van Geem, *Waste Management*, 2017, **69**, 24-58.
7. Thomas Hundertmark, Mirjam Mayer, Chris McNally, Theo Jan Simons and C. Witte, *How plastics waste recycling could transform the chemical industry*, McKinsey & Company, 2018.
8. M. Kusenberg, A. Eschenbacher, M. R. Djokic, A. Zayoud, K. Ragaert, S. De Meester and K. M. Van Geem, *Waste Management*, 2022, **138**, 83-115.
9. S. Dong, T. Ryu, C. Oi, J. Wu, N. R. Altvater, R. Hagmann, Z. Alikhani, E. A. Lebrón-Rodríguez, J. H. Jansen, V. S. Cecon, G. W. Curtzwiler, K. L. Vorst, G. W. Huber and I. Hermans, *Chemical Engineering Journal*, 2024, **482**, 148889.
10. H. Li, J. Wu, Z. Jiang, J. Ma, V. M. Zavala, C. R. Landis, M. Mavrikakis and G. W. Huber, *Science*, 2023, **381**, 660-666.
11. H. Li, A. Cutherbertson, A. A. Alamer, V. S. Cecon, H. Radhakrishnan, J. Wu, G. W. Curtzwiler, K. L. Vorst, X. Bai, C. R. Landis, G. T. Beckham and G. W. Huber, *Green Chemistry*, 2024, DOI: 10.1039/D4GC01013B.
12. M. Kusenberg, A. Zayoud, M. Roosen, H. D. Thi, M. S. Abbas-Abadi, A. Eschenbacher, U. Kresovic, S. De Meester and K. M. Van Geem, *Fuel Processing Technology*, 2022, **227**, 107090.
13. M. S. Abbas-Abadi, M. Kusenberg, A. Zayoud, M. Roosen, F. Vermeire, S. Madanikashani, M. Kuzmanović, B. Parvizi, U. Kresovic, S. De Meester and K. M. Van Geem, *Waste Management*, 2023, **165**, 108-118.
14. B. A. Perez and H. E. Toraman, *Journal of Analytical and Applied Pyrolysis*, 2024, **177**, 106376.
15. J. V. Jayarama Krishna, B. A. Perez and H. E. Toraman, *ACS Sustainable Chemistry & Engineering*, 2024, **12**, 7508-7518.
16. Y. Zhang, Z. Fu, W. Wang, G. Ji, M. Zhao and A. Li, *ACS Sustainable Chemistry & Engineering*, 2022, **10**, 91-103.
17. D. Zhao, X. Wang, J. B. Miller and G. W. Huber, *ChemSusChem*, 2020, **13**, 1764-1774.
18. M. J. Frisch, G. W. Trucks, H. B. Schlegel, G. E. Scuseria, M. A. Robb, J. R. Cheeseman, G. Scalmani, V. Barone, B. Mennucci, G. A. Petersson, H. Nakatsuji, M. Caricato, X. Li, H. P. Hratchian, A. F. Izmaylov, J. Bloino, G. Zheng, J. L. Sonnenberg, M. Hada, M. Ehara, K. Toyota, R. Fukuda, J. Hasegawa, M. Ishida, T. Nakajima, Y. Honda, O. Kitao, H. Nakai, T. Vreven, J. A. Montgomery Jr., J. E. Peralta, F. Ogliaro, M. J. Bearpark, J. J. Heyd, E. N. Brothers, K. N. Kudin, V. N. Staroverov, T. A. Keith, R. Kobayashi, J. Normand, K. Raghavachari, A. P. Rendell, J. C. Burant, S. S. Iyengar, J. Tomasi, M. Cossi, N. Rega, J. M. Millam, M. Klene, E. Knox, J. B. Cross, V. Bakken, C. Adamo, J. Jaramillo, R. Gomperts, R. E. Stratmann, O. Yazyev, A. J. Austin, R. Cammi, C. Pomelli, J. W. Ochterski, R. L. Martin, K. Morokuma, V. G. Zakrzewski, G. A. Voth, P. Salvador, J. J.

Dannenberg, S. Dapprich, A. D. Daniels, O. Farkas, J. B. Foresman, J. V. Ortiz and J. Cioslowski, *and D. J. Fox, Gaussian 09 (Gaussian, Inc., Wallingford CT, 2009)*.
19. L. K. Krehula, Z. Katančić, A. P. Siročić and Z. Hrnjak-Murgić, *Journal of Wood Chemistry and Technology*, 2014, **34**, 39-54.
20. G. S. Misra, *Introductory polymer chemistry*, New Age International, 1993.
21. J. Fang, L. Zhang, D. Sutton, X. Wang and T. Lin, *Journal of Nanomaterials*, 2012, **2012**, 382639.
22. J. Peyroux, M. Dubois, E. Tomasella, L. Frézet, A. P. Kharitonov and D. Flahaut, *European Polymer Journal*, 2015, **66**, 18-32.
23. Z. Wang, S. Li, B. Li, W. Lai, Y. Liu, Z. Cheng, X. Wang and X. Liu, *Journal of Fluorine Chemistry*, 2017, **200**, 169-178.
24. M. Pollard, K. Klimke, R. Graf, H. W. Spiess, M. Wilhelm, O. Sperber, C. Piel and W. Kaminsky, *Macromolecules*, 2004, **37**, 813-825.
25. Z. Zhou, S. Pesek, J. Klosin, M. S. Rosen, S. Mukhopadhyay, R. Cong, D. Baugh, B. Winniford, H. Brown and K. Xu, *Macromolecules*, 2018, **51**, 8443-8454.
26. L. A. Wall and S. Straus, *Journal of Polymer Science*, 1960, **44**, 313-323.
27. L. A. Wall, S. L. Madorsky, D. W. Brown, S. Straus and R. Simha, *Journal of the American Chemical Society*, 1954, **76**, 3430-3437.
28. I. Ahmad, M. I. Khan, H. Khan, M. Ishaq, R. Tariq, K. Gul and W. Ahmad, *International Journal of Green Energy*, 2015, **12**, 663-671.
29. H. Li, H. A. Aguirre-Villegas, R. D. Allen, X. Bai, C. H. Benson, G. T. Beckham, S. L. Bradshaw, J. L. Brown, R. C. Brown and V. S. J. G. C. Cecon, 2022, **24**, 8899-9002.
30. R. E. Harmon, G. SriBala, L. J. Broadbelt and A. K. Burnham, *Energy & Fuels*, 2021, **35**, 6765-6775.
31. T. Shiono, S. Yoshida, H. Hagihara and T. Ikeda, *Applied Catalysis A: General*, 2000, **200**, 145-152.
32. C. Maier and T. Calafut, in *Polypropylene*, eds. C. Maier and T. Calafut, William Andrew Publishing, Norwich, NY, 1998, DOI: https://doi.org/10.1016/B978-188420758-7.50006-0, pp. 3-9.
33. M. Tolinski, in *Additives for Polyolefins*, ed. M. Tolinski, William Andrew Publishing, Oxford, 2009, DOI: https://doi.org/10.1016/B978-0-8155-2051-1.00007-8, pp. 93-119.
34. P. Hiremath, K. Nuguru and V. Agrahari, in *Handbook of Pharmaceutical Wet Granulation*, eds. A. S. Narang and S. I. F. Badawy, Academic Press, 2019, DOI: https://doi.org/10.1016/B978-0-12-810460-6.00012-9, pp. 263-315.
35. M. Tolinski, in *Additives for Polyolefins*, ed. M. Tolinski, William Andrew Publishing, Oxford, 2009, DOI: https://doi.org/10.1016/B978-0-8155-2051-1.00009-1, pp. 137-156.
36. A. Ranji, M. Ghorbani Ravandi and M. A. Farajzadeh, *Analytical Sciences*, 2008, **24**, 623-626.
37. W. Zeb, M. Roosen, P. Knockaert, S. Janssens, D. Withoeck, M. Kusenberg, J. Hogie, P. Billen, S. Tavernier, K. M. Van Geem and S. De Meester, *Journal of Cleaner Production*, 2023, **416**, 137881.
38. J. A. González-Pérez, N. T. Jiménez-Morillo, J. M. de la Rosa, G. Almendros and F. J. González-Vila, *Journal of Chromatography A*, 2015, **1388**, 236-243.
39. V. V. Kislov, A. I. Sadovnikov and A. M. Mebel, *The Journal of Physical Chemistry A*, 2013, **117**, 4794-4816.
40. W. Hayduk and R. Castaneda, *The Canadian Journal of Chemical Engineering*, 1973, **51**, 353-358.
41. D. Fleury and W. J. T. C. J. o. C. E. Hayduk, 1975, **53**, 195-199.
42. C. T. Young, R. von Goetze, A. K. Tomov, F. Zaccaria and G. J. P. Britovsek, *Topics in Catalysis*, 2020, **63**, 294-318.
43. G. J. P. Britovsek, R. Malinowski, D. S. McGuinness, J. D. Nobbs, A. K. Tomov, A. W. Wadsley and C. T. Young, *ACS Catalysis*, 2015, **5**, 6922-6925.
44. P. A. Cuello-Penaloza, R. G. Dastidar, S.-C. Wang, Y. Du, M. P. Lanci, B. Wooler, C. E. Kliewer, I. Hermans, J. A. Dumesic and G. W. Huber, *Applied Catalysis B: Environmental*, 2022, **304**, 120984.

45. V. J. Triacca, P. E. Gloor, S. Zhu, A. N. Hrymak and A. E. Hamielec, *Polymer Engineering & Science*, 1993, **33**, 445-454.
46. D. Browarzik and A. Koch, *Journal of Macromolecular Science, Part A*, 1996, **33**, 1633-1641.
47. T. Ueno, E. Nakashima and K. Takeda, *Polymer Degradation and Stability*, 2010, **95**, 1862-1869.
48. H. Bockhorn, A. Hornung, U. Hornung and D. Schawaller, *Journal of Analytical and Applied Pyrolysis*, 1999, **48**, 93-109.
49. M. Seeger and H. J. Cantow, *Die Makromolekulare Chemie*, 1975, **176**, 2059-2078.
50. B. Dickens, *Journal of Polymer Science: Polymer Chemistry Edition*, 1982, **20**, 1169-1183.
51. L. Zhao, Z. Guo, S. Ran, Z. Cao and Z. Fang, *Journal of Thermal Analysis and Calorimetry*, 2014, **115**, 1235-1244.
52. A. Dhar, R. L. Vekariya and P. Bhadja, *Cogent Chemistry*, 2018, **4**, 1514686.
53. V. Ambrogi, C. Carfagna, P. Cerruti and V. Marturano, in *Modification of Polymer Properties*, eds. C. F. Jasso-Gastinel and J. M. Kenny, William Andrew Publishing, 2017, DOI: https://doi.org/10.1016/B978-0-323-44353-1.00004-X, pp. 87-108.
54. Y. Schächter and H. Pines, *Journal of Catalysis*, 1968, **11**, 147-158.

The data supporting the results of this study are included within the manuscript and in the supplementary information (ESI). For any further data requests, please reach out to the corresponding author. Your inquiry will be promptly addressed to enhance the understanding of the research.